Research, Society and Development, v. 9, n. 10, e7919109123, 2020
(CC BY 4.0) | ISSN 2525-3409 | DOI: http://dx.doi.org/10.33448/rsd-v9i10.9123

Synthesis and characterization of an experimental 3Y-TZP dental ceramic prepared by polymeric precursors method

Síntese e caracterização de uma cerâmica dentária experimental 3Y-TZP preparada pelo método de precursores poliméricos

Propiedades térmicas, estructurales y morfológicas de una cerámica dental experimental 3Y-TZP sintetizada por el método de precursores poliméricos

Received: 10/07/2020 | Reviewed: 10/13/2020 | Accept: 10/16/2020 | Published: 10/18/2020

Fabíola Stahlke Prado
ORCID: https://orcid.org/0000-0002-1594-2426
University of North Paraná, Brazil
E-mail: fabiola_stahlkeprado@hotmail.com
Tânia Cristina Simões
ORCID: https://orcid.org/0000-0002-9918-8685
Federal Institute of Paraná, Brazil
E-mail: tania.simoes@ifpr.edu.br
Alejandra Hortencia Miranda González
ORCID: https://orcid.org/0000-0003-2982-8736
University of North Paraná/ Anhanguera University of São Paulo, Brazil
E-mail: alejandra.horten@uol.com

Abstract

The aim of the investigation was to synthesize 3 mol% yttria-stabilized zirconia (3Y-TZP) powders via polymeric precursor method (PPM). The precursor solution was preheated at 350ºC for 3h, subsequently thermally treated at 500ºC for 3h and 800ºC for 6h. The obtained materials were analyzed by Thermogravimetry-Derivative Thermogravimetry (TG/DTG), Differential Thermal Analysis (DTA), powder X-ray Diffraction (XRD) and Scanning Electron Microscopy (SEM). Two commercially available Y-TZP ceramic systems were chosen for comparison. XRD analysis of the synthesized 3Y-TZP powders revealed the crystallization of the tetragonal phase, while both commercial systems showed the coexistence of the monoclinic and tetragonal phases. SEM analysis showed that the powders thermally treated at 800°C consist of agglomerated spherical nanoparticles. Morphology of commercial systems also revealed nanosized spherical particles. Results revealed that the

PPM led to ceramics with structural and morphological properties comparable to commercially available reinforced dental ceramics.

Keywords: Ceramics; 3Y-TZP; Chemical synthesis; Thermogravimetry; X-ray Diffraction; Scanning electron microscopy.

Resumo

O objetivo da pesquisa foi sintetizar pós de zircônia estabilizada com 3 mol% de ítria (3Y-TZP) por meio do método de precursores poliméricos (MPP). A solução precursora foi pré-aquecida a 350ºC por 3h, posteriormente tratada termicamente a 500ºC por 3h e 800ºC por 6h. Os materiais obtidos foram analisados por Termogravimetria – Termogravimetria Derivada (TG / DTG), Análise Térmica Diferencial (DTA), Difração de raios-X (DRX) e Microscopia Eletrônica de Varredura (MEV). Dois sistemas cerâmicos Y-TZP comercialmente disponíveis foram escolhidos para comparação. A análise de DRX dos pós sintetizados de 3Y-TZP revelou a cristalização da fase tetragonal, enquanto ambos os sistemas comerciais mostraram a coexistência das fases monoclínica e tetragonal. A análise de MEV mostrou que os pós tratados termicamente a 800ºC consistem em nanopartículas esféricas aglomeradas. A morfologia dos sistemas comerciais também revelou partículas esféricas nanométricas. Os resultados revelaram que o MPP produziu cerâmicas com propriedades estruturais e morfológicas comparáveis às cerâmicas odontológicas reforçadas disponíveis comercialmente.

Palavras-chave: Cerâmica, 3Y-TZP; Síntese química; Termogravimetria; Difração de raios X; Microscopia eletrônica de varredura.

Resumen

El objetivo de la investigación fue sintetizar polvos de zirconia estabilizada con itria al 3% molar (3Y-TZP) mediante el método de precursores poliméricos (MPP). La solución precursora se precalentó a 350ºC durante 3 h, posteriormente se trató térmicamente a 500ºC durante 3 h y 800ºC durante 6 h. Los materiales obtenidos se analizaron por Termogravimetría – Termogravimetría Diferencial (TG / DTG), Análisis Térmico Diferencial (DTA), Difracción de rayos X (DRX) y Microscopía Electrónica de Barrido (MEB). Se eligieron dos sistemas cerámicos Y-TZP disponibles comercialmente para la comparación. El análisis de DRX de los polvos de 3Y-TZP sintetizados reveló la cristalización de la fase tetragonal, mientras que ambos sistemas comerciales mostraron la coexistencia de las fases monoclínica y tetragonal. El análisis de MEB mostró que los polvos tratados térmicamente a

800ºC consisten en nanopartículas esféricas aglomeradas. La morfología de los sistemas comerciales también reveló partículas esféricas de tamaño nanométrico. Los resultados revelaron que el MPP condujo a cerámicas con propiedades estructurales y morfológicas comparables a las cerámicas dentales reforzadas disponibles comercialmente.

Palabras clave: Cerámica dental; Síntesis química; Termogravimetría; Difracción de rayos X; Microscopía electrónica de barrido.

1. Introduction

Zirconia is a polymorph and its crystals can be organized in three different crystallographic phases: monoclinic phase (M), cubic phase (C) and tetragonal phase (T), which has mechanical properties improved (Garvie et al., 1975; Piconi & Maccauro, 1999). Pure zirconia is monoclinic at room temperature, remaining stable at that stage to the temperature of 1170°C. During the temperature range between 1170°C and 2370°C it enters the tetragonal phase and above 2370°C up to its melting point it is found in the cubic phase (Kelly & Denry, 2008; Chevalier & Gremillard, 2009).

The addition of 3 mol% of yttrium oxide allows the stabilization at room temperature of polycrystalline zirconia in its tetragonal phase (3Y-TZP). This zirconia has as favorable characteristics, the size of its grain, on the order of hundreds of nanometers, and the process of tenacification that inhibits the propagation of cracks (Miyazaki et al., 2013; Chevalier, 2006; Miragaya et al., 2017). Because of its superior mechanical properties, biocompatibility to human tissues and improved optical properties, 3Y-TZP ceramics have become increasingly important in recent decades as biomaterials for restorations, being widely used commercially in the manufacture of crowns, dental prostheses and implants (Pieralli et al., 2017; Denry & Kelly, 2008; Zhang & Lawn, 2019; Li et al., 2014; Afrashtehfar & Fabbro, 2019; Gautam et al., 2016). The final mechanical properties of Y-TZP ceramics depend on some parameters, including the fraction of grains retained in the tetragonal phase at room temperature that is depended on, the grain size and shape, yttria content, and the degree of restriction exerted on them by the matrix (Guazzato et al., 2004; Muñoz-Tabares et al., 2011; Zhang & Lawn, 2018; Uz et al., 2020).

It is important to consider that due to the metastable nature of the tetragonal grains there is a critical grain size, linked to the concentration of yttrium above which a spontaneous T $\rightarrow$ M transformation of the grain may occur. Thus, a fine grain structure can inhibit the occurrence of a possible spontaneous transformation (Quinelato et al., 2000; Chevalier et al.,

2004). Some important variables, however, influence the final mechanical properties and microstructure of the ceramic, such as, synthesis and processing methodology used, quantity and types of additives, as well as the heat treatment during sintering process (Presenda et al., 2015; Retamal et al., 2016; Soubelet et al., 2018; Stawarczyk et al., 2012).

The polymer precursor method (PPM), also known as the Pechini method, consists of a chemical route used to produce ceramic powders. This method offers several advantages in the processing of powders, such as steps that allow stoichiometric control, lower synthesis temperatures, possibility to work in aqueous solution and not require special care with the atmosphere, besides the possibility of producing powders with nanometric particle size (Quinelato et al., 2000; Li et al., 2019; Sangeetha et al., 2019).

Thus, the aim of the present study was to synthesize 3Y-TZP powders by PPM to obtain a material with comparable characteristics with those presented by commercially available dental systems.

2. Methodology

This study describes an experimental quantitative, qualitative and descriptive research according to Pereira et al. (2018), that is pointed out by a morphological and structural characterization of an experimental and commercial ceramics.

Production of 3Y-TZP experimental powder

The PPM was employed for synthesis of the 3 mol% yttria-stabilized zirconia powders (3Y-TZP). This method is based on metallic citrate polymerization with the use of ethylene glycol. Polymerization, promoted by heating of the mixture, results in a homogeneous resin in which the metal ions are uniformly distributed throughout the organic matrix. A solution of 80% in mass of zirconium butoxide in butanol, ($Zr(OC_4H_9)_4$, Aldrich), and yttrium nitrate hexahydrate, ($Y(NO_3)_3.6H_2O$, Aldrich), were utilized as raw materials. The preparation involved the following steps: complexation reaction of metal ions with citric acid anhydrous ($C_6H_8O_7$, Synth) and esterification reaction promoted by Ethylene glycol ($C_2H_6O_2$, Synth). Gravimetric analyses were performed in triplicate to determine the Zr^{4+} ion concentration in the polymeric resin. Finally, a stoichiometric quantity of $Y(NO_3)_3.6H_2O$ was added to achieve a solution containing 3 mol% yttria-zirconia. The mixture was kept stirring and prolonged heating at 130ºC for 1 h produced a viscous transparent resin. Charring the resin at 350°C for

3 h in a box furnace resulted in a black solid mass, experimental powder (EP350), which was characterized by means of TG/DTG and DTA. The experimental powder was finally undergoing a heat treatment at 500°C for 3h (EP500) and then at 800°C for 6 h (EP800), in static air, to reach the crystallization stage as described in Table 1. 3Y-TZP powders were characterized by XRD to evaluate crystalline phases. The powder obtained from the heat treatment at 800°C for 6 h was also analyzed by SEM.

Table 1- Description of 3Y-TZP experimental powders.

Code	Material	Heat Treatment		Characterizations
		Initial	Final	
EP350	3Y-TZP experimental powder	350°C/3 h	-	TG/DTG, DTA, XRD
EP500	3Y-TZP experimental powder	350°C/3 h	500°C/3 h	XRD
EP800	3Y-TZP experimental powder	350°C/3 h	800°C/6 h	XRD, SEM

Source: Elaborated by the authors (2020).

Processing of commercial dental ceramics

Pre-sintered dental ceramic compacts of VITA InCeram® YZ (VT) and Ceramill® zirconia (CZ) were cut as blocks with a diamond wafering disc mounted on a specific cutter machine (Isomet 1000, Buehler, Lake Bluff, IL, USA) and disaggregated with the aid of a mortar and pestle. A detailed description of these materials is listed in Table 2. The commercial powders thus obtained were analyzed by XRD and SEM.

Table 2- Description of commercial dental materials used in this study.

Code	Commercial name	Manufacturer	Chemical composition % by weight
VT	VITA In-Ceram® YZ	VITA Zahnfabrik H. Rauter GmbH & Co. KG, Bad Säckingen, Germany	ZrO_2: ≥ 95 Y_2O_3: 5 HfO_2: < 3 $Al_2O_3 + SiO_2$: < 1
CZ	Ceramill® zirconia	Amann Girrbach AG, Koblach, Austria	$ZrO_2 + HfO_2 + Y_2O_3$: ≥ 99,0 Y_2O_3: 4,5 – 5,6 HfO_2: ≤ 5 Al_2O_3: ≤ 0,5 Other oxides: ≤ 1

Source: Manufacture's information.

Characterization

TG and DTA analyses were simultaneously used for thermal characterization of the experimental powder, EP350. Approximately 80 mg of the sample was placed in standard NETZSCH alumina 85 mL crucible attached to a thermoanalytical unit (TGA-50 Netzsch-Thermische Analyse, Selb, Germany) with a TA System Controller (TASC 414/2), a temperature range of 25–1300°C, at a heating rate of 10°C/min, and under dynamic nitrogen atmosphere (50 mL/min). TG measured the change in mass of the sample as a function of temperature. In DTA, the experimental powder and the inert reference underwent identical thermal cycles, while recording any temperature differences between sample and reference. This differential temperature of EP350 group was plotted against heating. Changes in temperature, either exothermic or endothermic, were detected relative to reference. The baseline to correct thermo-analytical curves was also performed for both analyses using empty alumina crucibles under the same experimental conditions.

XRD analyses were carried out with a Rigaku Miniflex600 X-ray diffractometer (Rigaku International Corporation,Tokyo, Japan) using CuKα radiation source (λ = 1.54056 Å) operating at 40 kV and 15 mA. Scans were performed from 10° to 80° (2θ) at a step size of 0.02° with a scan speed of 2°/min. Qualitative phase analysis was performed by using the Joint Committee on Powder Diffraction – International Center for Diffraction Data (JCPDS–

ICDD) databases. The average crystallite size of the samples was derived from XRD data using Scherrer equation (Zsigmondy & Scherrer, 1912).

Prior to SEM analyses 10 mg of each ceramic powder was diluted in 10 mL of ethanol absolute in a test tube. Then, the test tubes were taken into an ultrasonic vat and held for 15 min. After this process, with a pipette aid, a drop of each mixture was deposited individually on silicon substrates, which were fixed on stubs with double face carbon tape and desiccated in silica gel for 2 h. The specimens were then sputtered (Q150R Plus - Rotary pumped coater, Quorum Technologies Ltd., East Sussex, United Kingdom) with a thin gold film for 100 s at 40 mA and examined by a scanning electron microscope. SEM micrographs were recorded in the secondary electron mode on a ZEISS EVO LS15 Scanning Electron Microscope (Carl Zeiss, Germany) set at an acceleration tension of 10 kV.

3. Results and Discussion

Thermal analyses

Simultaneous measurements of thermogravimetric and differential thermal analyses were carried out for experimental powder, EP350. Displayed in Fig. 1 are the TG/DTG curves plotted against temperature. Thermal analysis demonstrated that weight loss occurred in two well-defined stages. The first one (25– 245ºC), was accompanied by a weight loss of 5.0 %, and was associated to water and solvent evaporation and to desorption of the gas adsorbed on powder surface. The second and more significant weight loss stage (13.8%) took place from 245 to 1300ºC and was related to the decomposition of polyester chain and carboxyl groups linked to metal with a consequent formation of crystalline metal-oxygen phase (Fernandes et al., 2018; Zhang et al., 2020; Kuo et al., 2011; Shi et al., 2014).

Figure 1- TG/DTG curves of 3Y-TZP experimental powder.

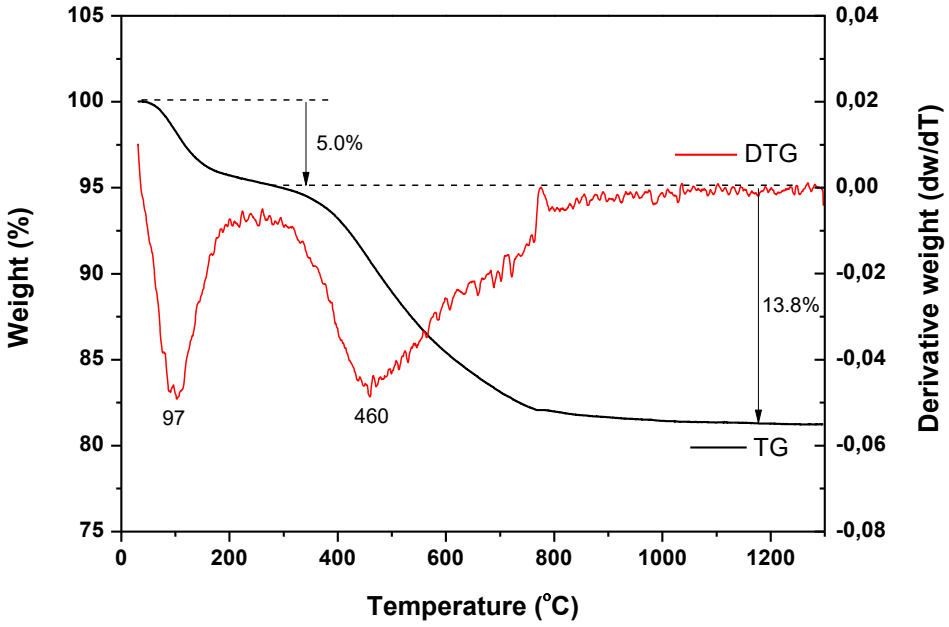

Source: Elaborated by the authors (2020).

DTA curve (Fig. 2) shows both endothermic and exothermic processes involved in decomposition of the polyester.

Figure 2- DTA curve of 3Y-TZP experimental powder.

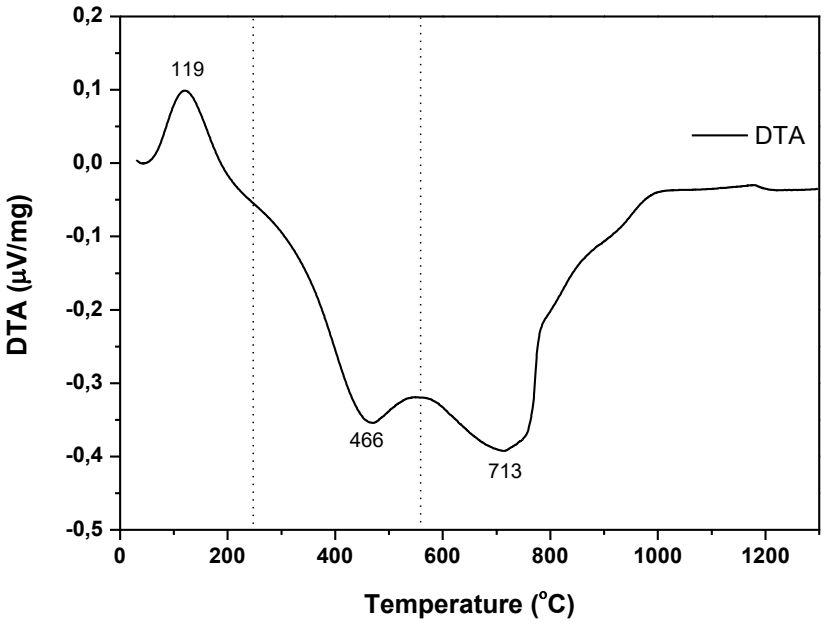

Source: Elaborated by the authors (2020).

The first endothermic range between 25°C and 245°C can be related to physical desorption and loss of ethylene glycol and water molecules. The exothermic DTA peak at 466ºC can be related to decomposition of polyester chain and formation of metal-oxygen bonds, leading to crystallization of 3Y-TZP phase. Therefore, this exothermic peak may be responsible for transformation from amorphous to tetragonal crystalline structure (Shi, 2014; Kuo, 2011), which can be confirmed by the fact XRD diffraction peaks of experimental powder thermally treated at 500ºC for 3h (EP500) corresponding to tetragonal phase as shown in Fig. 3. The second DTA peak at 713ºC can be assigned to a crystalline phase arrangement.

X-ray diffraction analyses

Diffraction patterns of 3Y-TZP experimental powders synthesized via PPM and thermally treated at different temperature conditions are displayed at Fig. 3.

Figure 3- XRD patterns of 3Y-TZP experimental powders. * t(*h k l*) means tetragonal crystalline planes of 3Y-TZP.

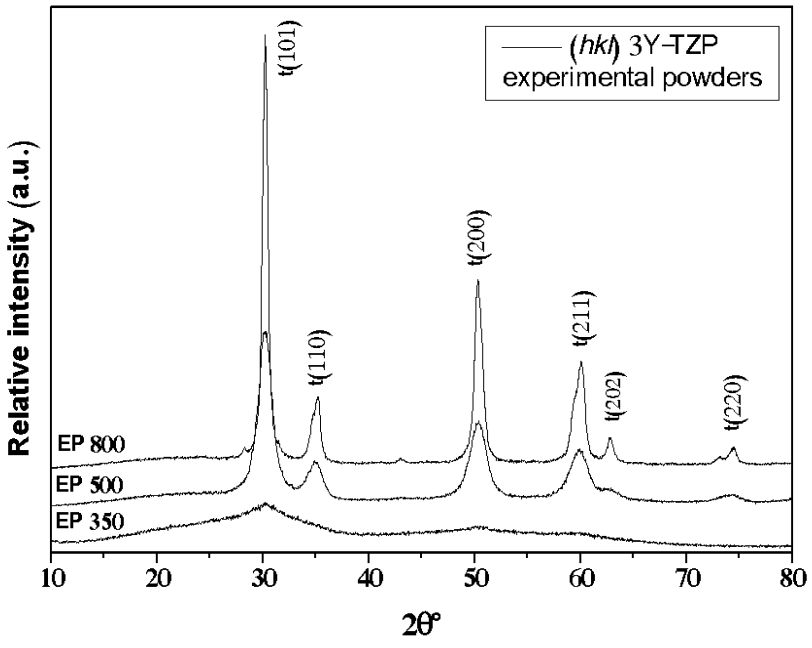

Source: Elaborated by the authors (2020).

EP 350 sample showed a brown color indicating a large amount of carbon, confirmed by amorphous profile revealed in diffractogram. Therefore, heating treatment at 350ºC for 3 h was insufficient to ensure complete decomposition of organic binders (Maritan et al., 2006;

Silva et al., 2019). XRD analysis of experimental powder treated at 500°C for 3 h (EP500) confirmed the beginning of the crystallization process. However, visual analysis showed a greyish color, indicating that the temperature was not enough to guarantee the complete crystallization. At 800°C (EP800) a white powder was obtained, characteristic of the complete decomposition of organic material. XRD pattern indicated well-defined crystallographic peaks reflecting the high crystallinity of the tetragonal phase. Thus, considering high crystallinity of the powder heated at 800°C for 6 h, this thermal treatment condition was adopted as the most suitable for obtaining pre-sintered experimental 3Y-TZP powders.

In addition to rise of heat, it was observed diffraction peaks intensity increasement, which confirms tetragonal phase stabilization. Highest intensity peaks identified in 2θ = 30.2°, 35.0°, 50.2°, 60.0°, 62.8° and 74.4°, related to (101), (110), (200), (211), (202) and (220) planes respectively, were associated only to crystallization of tetragonal phase. No peak associated with the monoclinic crystalline phase was identified.

All peaks and associated planes of 3Y-TZP diffractograms observed agree with the crystallographic data sheet, 791769, of tetragonal zirconia, ZrO_2, obtained from PCPDFWIN database of *International Centre for Diffraction Data* (ICDD). In accordance with database, pattern has a tetragonal cell with the following parameters: a = 3.595 Å and c = 5.185 Å.

Synthesis of 3Y-TZP carried out by a homogeneous precipitation process and preheated at 400°C reported by Oliveira et al, showed crystallization of the tetragonal phase. However, between 400°C and 650°C coexistence of tetragonal and monoclinic phases was verified and above 650°C it was 100% monoclinic (Oliveira & Torem, 2001).

Commercially powders VT and CZ were characterized by XRD in order to evaluate their crystallinity (Fig. 4). The analysis of the crystalline phases, as well as assignment of crystallographic planes was performed using crystallographic records 79-1769 (tetragonal ZrO_2) and 89-9066 (monoclinic ZrO_2) from the PCPDFWIN database as reference.

Figure 4- XRD patterns of Y-TZP powders: (a) EP800; (b) VT; (c) CZ. * t(*h k l*) means tetragonal crystalline planes and m(*h k l*) means monoclinic crystalline planes.

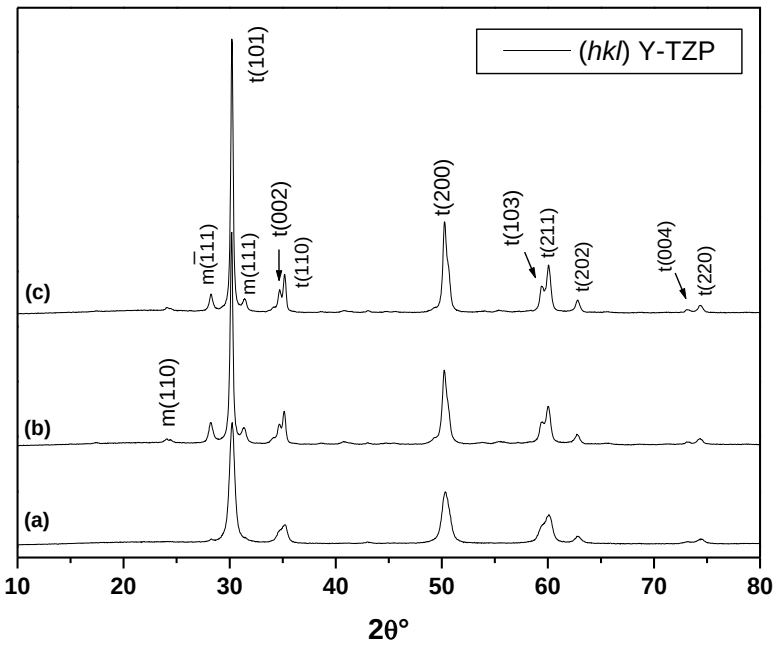

Source: Elaborated by the authors (2020).

XRD pattern for EP800 sample analyzed in comparison to patterns presented by VT and CZ systems indicated the effective crystallization of tetragonal phase in both groups. However, contrary to what was expected, for the commercial systems, deleterious monoclinic phase was also confirmed. In different circumstances, Arata et al. described the presence of tetragonal phase only on the quantitative XRD analysis of VITA In-Ceram® YZ system (Arata et al., 2014). The same results were achieved by Lazar et al. which synthesized 3Y-TZP powders by means of a chemical coprecipitation route. In that study, characterization by XRD revealed a phase content of 96% tetragonal and 4% monoclinic (Lazar et al., 2008). In another study, synthesis of 3Y-TZP powders was carried out by several processes, including microemulsion, ultrasound and lyophilization. After crystallization XRD results indicated that powders consisted mainly of tetragonal phase. On the other hand, a small amount of unreacted cubic Y_2O_3 was also identified (Liang et al., 2008). Similar result was described after the synthesis of Y-TZP powders doped with 8 mol% of Y_2O_3 and led to cubic phase crystallization of ZrO_2 (Ojha et al., 2010).

By alloying zirconia with stabilizers, as yttria (Y_2O_3), the tetragonal (T) form of metastable zirconia at room temperature could be achieved (Kim, 2020). In response to tensile stresses at crack-tips, stabilized tetragonal zirconia transforms to a more stable monoclinic

phase with a local increase in volume of approximately 4–5%. Toughening mechanism is based on a spontaneous stress-induced martensitic transformation at the crack-tip shielding (Cottom & Mayo, 1996; Studart et al., 2007; Xue et al., 2020). Y-TZP materials contain between 1.5 and 3.5 mol% Y_2O_3 in solid solution as phase stabilizer, this range allows to almost 100% tetragonal phase content (Miyazaki et al., 2013). Biomedical grade zirconia usually contains 3 mol% Y_2O_3 as a stabilizer (3Y-TZP) (Piconi & Maccauro, 1999), which possesses superior mechanical properties due to its relatively fine grain size (Kelly & Denry, 2008; Stawarczyk et al., 2012; Presenda et al., 2015). There is a strong dependence of the grain size with the transformation toughening effect in zirconia materials. From Y-TZP powders may be obtained very fine grain microstructures (particle size of 0.5 μm) (Piconi & Maccauro, 1999). It is known that 3Y-TZP particles is less stable above a critical grain size (<1 μm) and more susceptible to spontaneous T → M transformation. While smaller grain sizes are associated with a lower transformation rate. Moreover, below a certain grain size (~0.2 μm) leads to a reduction on fracture toughness, just because the transformation is not possible (Denry & Kelly, 2008; Cottom & Mayo, 1996; Bravo-Leon et al., 2002).

The traditional tool used to determine the size of the crystallites from XRD data is Scherrer equation (1):

$$D_{h\,k\,l} = \frac{K\lambda}{\beta_{h\,k\,l}\cos\theta_{h\,k\,l}} \quad (1)$$

where $D_{h\,k\,l}$ is the so-called average crystallite size, K is a constant depending on particle shape and assumed to be equal to 0.9, λ is a wavelength of X-rays (1.54060 Å), $\beta_{h\,k\,l}$ is the full width at half maximum (FWHM) of the peak in rad and $\theta_{h\,k\,l}$ is a position of the peak.

The average crystallite size of Y-TZP powders was calculated from standard peaks and is represented in Table 3. Size calculated from the Scherrer equation was 13.85 nm (EP800), 27.24 nm (VT) and 31.43 nm (CZ). Thus, the value of crystal size determined from X-ray data of synthesized 3Y-TZP was in good agreement with those presented by commercial dental systems.

Table 3- Average crystallite size of Y-TZP powders calculated from the Scherrer equation.

Sample	FWHM (2θ)	Average crystallite size (nm)
EP800	0.591	13.85
VT	0.301	27.24
CZ	0.260	31.43

Source: Elaborated by the authors (2020).

SEM analyses

Representative SEM analyses are presented in Fig. 5 (from A to C). Illustrations revealed that there was great variability in terms of shape and size of the particles present in Y-TZP samples tested. From characterization of EP800 by SEM (Fig. 5A) it was verified that morphology consisted of agglomerated spherical nanosized grains. The agglomerates formed, due to the high surface area, were larger than those presented by VT and CZ groups, as shown in Fig. 5B and 5C, respectively.

Figure 5- SEM micrographs of Y-TZP powders: (A) EP800; (B) VT; (C) CZ. Magnification 15000x.

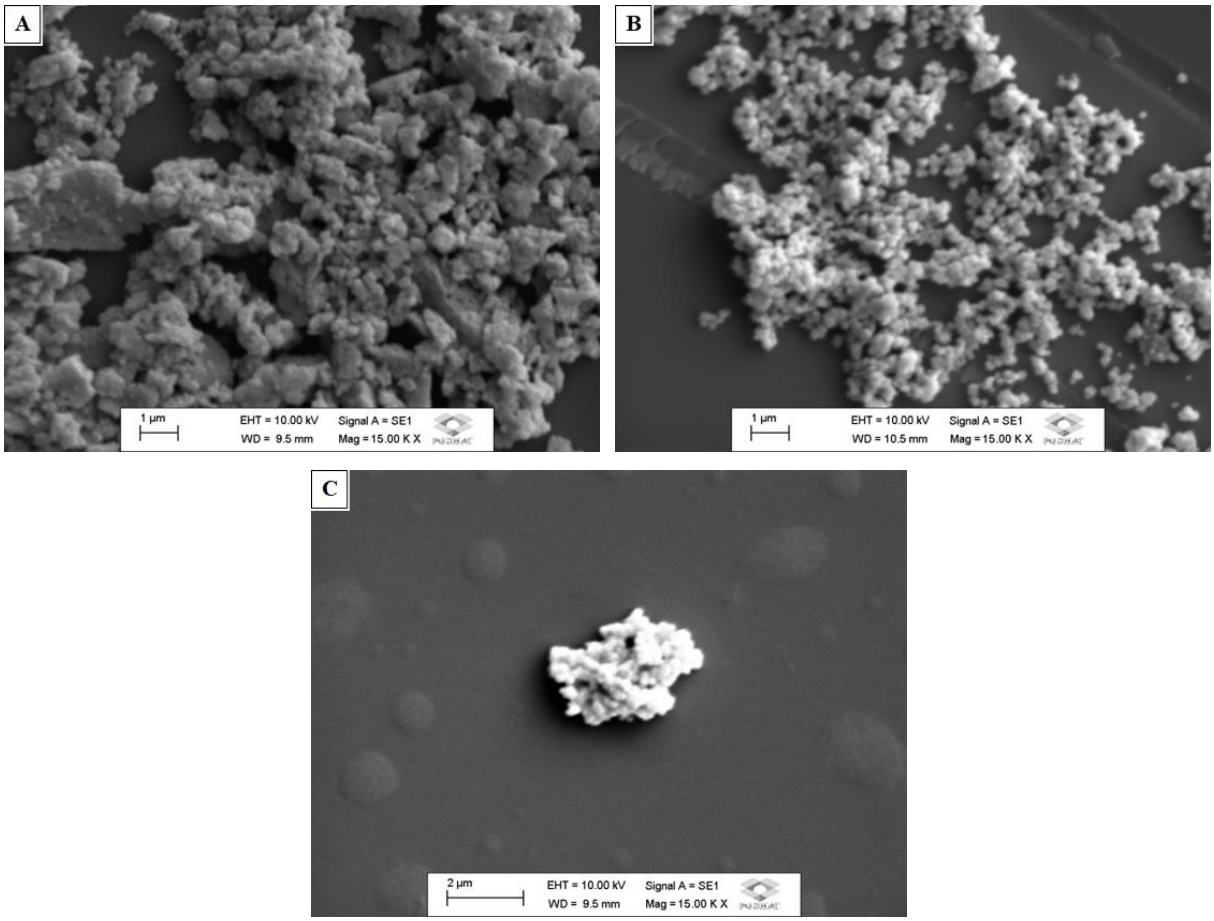

Source: Elaborated by the authors (2020).

In both commercial systems, morphology analyses revealed small homogeneous particles with size related to nanoparticles. Images also revealed that VT system presented particles with more homogeneous distribution in terms of size and shape.

Some studies have reported similar morphology for powders prepared by other chemical routes (Díaz-Parralejo et al., 2011). 3Y-TZP powders prepared by a microemulsion route revealed particles with diameters of 29-33 nm (Liang et al., 2008). Y-TZP crystals synthesized by hydrothermal method, doped with 3 to 9 mol% of Y_2O_3, presented nanometric agglomerates with particle sizes ranging from 4-6 nm (Hayashi et al., 2009). In another study, SEM images revealed clearly visible outlines grains with irregular size. Although the average grain size was calculated to be 0.47 µm, many wide grains larger than 1 µm were identified (Tong et al., 2016).

Therefore, from the results obtained in the present study, crystallization process of 3Y-TZP powders revealed 100% tetragonal crystalline phase. Thus, it was confirmed the

efficiency of chemical synthesis by PPM ensuring that monoclinic phase crystallization did not occur during heat treatment. In addition, morphological properties of 3Y-TZP experimental powders synthesized, which consisted of clusters formed by spherical particles, can be related to the high surface area of the ceramic nanoparticles. These properties were found to be comparable to those of similar materials prepared by other chemical routes and solid-state reaction methods.

4. Conclusions

As anticipated, the choice of PPM as a chemical route proved to be efficient in producing crystalline and single-phase 3Y-TZP ceramic powders. Thermal behavior revealed a weight loss of 18.8% involved in decomposition of polyester chain. Exothermic process at 466ºC confirmed the crystallization of 3Y-TZP phase. Considering the heat treatment conditions studied, powder thermally heated at 800ºC for 6 h presented high crystallinity of tetragonal phase. Also, as compared to commercial dental systems, 3Y-TZP experimental powder revealed the same order of particle size. From the general analysis of SEM results it was concluded once again that PPM has been shown to be efficient in synthesis of homogeneous and nanostructured powders. Therefore, further studies evaluating the mechanical and biological properties will be carried out.

Acknowledgments

This study was supported by the Coordenação de Aperfeiçoamento de Pessoal de Nível Superior - Brasil (CAPES). Authors are also grateful to Prof. Dayse Iara dos Santos, Prof. Fenelon Martinho Lima Pontes and Prof. Luís A. Sousa Marques da Rocha from School of Sciences – UNESP/Bauru, for their support in Thermal, XRD and SEM analyses, respectively.

References

Afrashtehfar, K. I., & Fabbro, M. Del. (2019). Clinical performance of zirconia implants : A meta-review. *The Journal of Prosthetic Dentistry*, *123*(3), 419–426. https://doi.org/10.1016/j.prosdent.2019.05.017

Arata, A., Campos, T. M. B., Machado, J. P. B., Lazar, D. R. R., Ussui, V., Lima, N. B., & Tango, R. N. (2014). Quantitative phase analysis from X-ray diffraction in Y-TZP dental ceramics: A critical evaluation. *Journal of Dentistry*, *42*(11), 1487–1494. https://doi.org/10.1016/j.jdent.2014.08.010

Bravo-Leon, A., Morikawa, Y., Kawahara, M., & Mayo, M. J. (2002). Fracture toughness of nanocrystalline tetragonal zirconia with low yttria content. *Acta Materialia*, *50*(18), 4555–4562. https://doi.org/10.1016/S1359-6454(02)00283-5

Chevalier, J., & Gremillard, L. (2009). Ceramics for medical applications: A picture for the next 20 years. In *Journal of the European Ceramic Society* (Vol. 29, Issue 7, pp. 1245–1255). https://doi.org/10.1016/j.jeurceramsoc.2008.08.025

Chevalier, J. (2006). What future for zirconia as a biomaterial? *Biomaterials*, *27*(4), 535–543. https://doi.org/10.1016/j.biomaterials.2005.07.034

Chevalier, J., Deville, S., Münch, E., Jullian, R., & Lair, F. (2004). Critical effect of cubic phase on aging in 3 mol% yttria-stabilized zirconia ceramics for hip replacement prosthesis. *Biomaterials*, *25*(24), 5539–5545. https://doi.org/10.1016/j.biomaterials.2004.01.002

Cottom, B. A., & Mayo, M. J. (1996). Fracture toughness of nanocrystalline ZrO2-3mol% y2o3 determined by vickers indentation. *Scripta Materialia*, *34*(5), 809–814. https://doi.org/10.1016/1359-6462(95)00587-0

Denry, I., & Kelly, J. R. (2008). State of the art of zirconia for dental applications. *Dental Materials*, *24*(3), 299–307. https://doi.org/10.1016/j.dental.2007.05.007

Díaz-Parralejo, A., Cuerda-Correa, E. M., Macías-García, A., Díaz-Díez, M. A., & Sánchez-González, J. (2011). Tailoring the properties of yttria-stabilized zirconia powders prepared by the sol-gel method for potential use in solid oxide fuel cells. *Fuel Processing Technology*, *92*(2), 183–189. https://doi.org/10.1016/j.fuproc.2010.05.033

Fernandes, S. L., Gasparotto, G., Teixeira, G. F., Cebim, M. A., Longo, E., & Zaghete, M. A.

(2018). Lithium lanthanum titanate perovskite ionic conductor: Influence of europium doping on structural and optical properties. *Ceramics International*, *44*(17), 21578–21584. https://doi.org/10.1016/j.ceramint.2018.08.221

Garvie, R. C., Hannink, R. H., & Pascoe, R. (1975). Ceramic steel? *Nature*, *258*(1), 703–704.

Gautam, C., Joyner, J., Gautam, A., Rao, J., & Vajtai, R. (2016). Zirconia based dental ceramics: structure, mechanical properties, biocompatibility and applications. *Dalton Transactions*, *45*(48). https://doi.org/10.1039/c6dt03484e

Guazzato, M., Albakry, M., Ringer, S. P., & Swain, M. V. (2004). Strength, fracture toughness and microstructure of a selection of all-ceramic materials. Part II. Zirconia-based dental ceramics. *Dental Materials*, *20*(5), 449–456. https://doi.org/10.1016/j.dental.2003.05.002

Hayashi, H., Ueda, A., Suino, A., Hiro, K., & Hakuta, Y. (2009). Hydrothermal synthesis of yttria stabilized ZrO2 nanoparticles in subcritical and supercritical water using a flow reaction system. *Journal of Solid State Chemistry*, *182*(11), 2985–2990. https://doi.org/10.1016/j.jssc.2009.08.013

Kelly, J. R., & Denry, I. (2008). Stabilized zirconia as a structural ceramic: An overview. *Dental Materials*, *24*(3), 289–298. https://doi.org/10.1016/j.dental.2007.05.005

Kim, H. (2020). E ff ect of A Rapid-Cooling Protocol on the Optical and Mechanical Properties of Dental Monolithic Zirconia. *Materials*, *13*(1923). https://doi.org/10.3390/ma13081923

Kuo, C. W., Shen, Y. H., Wen, S. B., Lee, H. E., Hung, I. M., Huang, H. H., & Wang, M. C. (2011). Phase transformation kinetics of 3 mol% yttria partially stabilized zirconia (3Y-PSZ) nanopowders prepared by a non-isothermal process. *Ceramics International*, *37*(1), 341–347. https://doi.org/10.1016/j.ceramint.2010.09.018

Lazar, D. R. R., Bottino, M. C., Özcan, M., Valandro, L. F., Amaral, R., Ussui, V., & Bressiani, A. H. A. (2008). Y-TZP ceramic processing from coprecipitated powders: A

comparative study with three commercial dental ceramics. *Dental Materials*, *24*(12), 1676–1685. https://doi.org/10.1016/j.dental.2008.04.002

Li, R. W. K., Chow, T. W., & Matinlinna, J. P. (2014). Ceramic dental biomaterials and CAD/CAM technology: State of the art. *Journal of Prosthodontic Research*, *58*(4), 208–216. https://doi.org/10.1016/j.jpor.2014.07.003

Li, X., Qian, J., Xu, J., Sun, Y., & Liu, L. (2019). Synthesis and electrical properties of antimony–doped tin oxide–coated TiO 2 by polymeric precursor method. *Materials Science in Semiconductor Processing*, *98*(March), 70–76. https://doi.org/10.1016/j.mssp.2019.03.024

Liang, X., Qiu, Y., Zhou, S., Hu, X., Yu, G., & Deng, X. (2008). Preparation and properties of dental zirconia ceramics. *Journal of University of Science and Technology Beijing: Mineral Metallurgy Materials (Eng Ed)*, *15*(6), 764–768. https://doi.org/10.1016/S1005-8850(08)60284-4

Maritan, L., Nodari, L., Mazzoli, C., Milano, A., & Russo, U. (2006). Influence of firing conditions on ceramic products: Experimental study on clay rich in organic matter. *Applied Clay Science*, *31*(1–2), 1–15. https://doi.org/10.1016/j.clay.2005.08.007

Miragaya, L. M., Guimarães, R. B., Souza, R. O. de A. e., Guimarães, J. G. A., & da Silva, E. M. (2017). Effect of intra-oral aging on t→m phase transformation, microstructure, and mechanical properties of Y-TZP dental ceramics. *Journal of the Mechanical Behavior of Biomedical Materials*, *72*, 14–21. https://doi.org/10.1016/j.jmbbm.2017.04.014

Miyazaki, T., Nakamura, T., Matsumura, H., Ban, S., & Kobayashi, T. (2013). Current status of zirconia restoration. *Journal of Prosthodontic Research*, *57*(4), 236–261. https://doi.org/10.1016/j.jpor.2013.09.001

Muñoz-Tabares, J. A., Jiménez-Piqué, E., Reyes-Gasga, J., & Anglada, M. (2011). Microstructural changes in ground 3Y-TZP and their effect on mechanical properties. *Acta Materialia*, *59*(17), 6670–6683. https://doi.org/10.1016/j.actamat.2011.07.024

Ojha, P. K., Rath, S. K., Chongdar, T. K., & Kulkarni, A. R. (2010). Nanocrystalline yttria

stabilized zirconia by metal-PVA complexation. *Ceramics International*, *36*(2), 561–566. https://doi.org/10.1016/j.ceramint.2009.09.035

Oliveira, A. P., & Torem, M. L. (2001). The influence of precipitation variables on zirconia powder synthesis. *Powder Technology*, *119*(2–3), 181–193. https://doi.org/10.1016/S0032-5910(00)00422-8

Pereira, A. S., Shitsuka, D. M., Parreira, F. J., & Shitsuka, R. (2018). Metodologia da pesquisa científica.[e-book]. Santa Maria. Ed. UAB/NTE/UFSM. Retrieved from https://repositorio. ufsm. br/bitstream/handle/1/15824/Lic_Computacao_Metodologia-Pesquisa-Cientifica.pdf. https://repositorio.ufsm.br/bitstream/handle/1/15824/Lic_Computacao_Metodologia-Pesquisa-Cientifica.pdf?sequence=1

Piconi, C., & Maccauro, G. (1999). Zirconia as a Dental Biomaterial. *Biomaterials*, *20*, 1–25. https://doi.org/10.3390/ma8084978

Pieralli, S., Kohal, R. J., Jung, R. E., Vach, K., & Spies, B. C. (2017). Clinical Outcomes of Zirconia Dental Implants: A Systematic Review. *Journal of Dental Research*, *96*(1), 38–46. https://doi.org/10.1177/0022034516664043

Presenda, Á., Salvador, M. D., Peñaranda-Foix, F. L., Moreno, R., & Borrell, A. (2015). Effect of microwave sintering on microstructure and mechanical properties in Y-TZP materials used for dental applications. *Ceramics International*, *41*(5), 7125–7132. https://doi.org/10.1016/j.ceramint.2015.02.025

Quinelato, A. L., Longo, E., Perazolli, L. A., & Varela, J. A. (2000). Effect of ceria content on the sintering of ZrO2 based ceramics synthesized from a polymeric precursor. *Journal of the European Ceramic Society*, *20*(8), 1077–1084. https://doi.org/10.1016/S0955-2219(99)00269-1

Retamal, C., Lagos, M., Moshtaghioun, B. M., Cumbrera, F. L., Domínguez-Rodríguez, A., & Gómez-García, D. (2016). A new approach to the grain-size dependent transition of stress exponents in yttria tetragonal zirconia polycrystals. the theoretical limit for superplasticity in

ceramics. *Ceramics International*, *42*(4), 4918–4923. https://doi.org/10.1016/j.ceramint.2015.12.005

Sangeetha, A., Chikkahanumantharayappa, & Nagabhushana, B. M. (2019). Comparative study of photoluminescence of single and mixed phase ZrTiO4 prepared by solution combustion and polymeric precursor method. *Journal of Molecular Structure*, *1179*, 126–131. https://doi.org/10.1016/j.molstruc.2018.10.059

Shi, L., Chen, W., Zhou, X., Zhao, F., & Li, Y. (2014). Pr-doped 3Y-TZP nanopowders for colored dental restorations: Mechanochemical processing, chromaticity and cytotoxicity. *Ceramics International*, *40*(6), 8569–8574. https://doi.org/10.1016/j.ceramint.2014.01.071

Silva, B. F., Maestrelli, S. C., Damasceno, L. H. S., Costa, R. B., Guarda, A. L., & Roveri, C. D. (2019). Ceramic characterization of raw material with a high content of organic matter reduced by composting. *Ceramica*, *65*, 34–39. https://doi.org/10.1590/0366-6913201965S12602

Soubelet, C. G., Albano, M. P., & Conconi, M. S. (2018). Sintering, microstructure and hardness of Y-TZP- 64S bioglass ceramics. *Ceramics International*, *44*(5), 4868–4874. https://doi.org/10.1016/j.ceramint.2017.12.076

Stawarczyk, B., Özcan, M., Hallmann, L., Ender, A., Mehl, A., & Hämmerlet, C. H. F. (2012). The effect of zirconia sintering temperature on flexural strength, grain size, and contrast ratio. *Clinical Oral Investigations*, *17*(1), 269–274. https://doi.org/10.1007/s00784-012-0692-6

Studart, A. R., Filser, F., Kocher, P., & Gauckler, L. J. (2007). Fatigue of zirconia under cyclic loading in water and its implications for the design of dental bridges. *Dental Materials*, *23*(1), 106–114. https://doi.org/10.1016/j.dental.2005.12.008

Tong, H., Tanaka, C. B., Kaizer, M. R., & Zhang, Y. (2016). Characterization of three commercial Y-TZP ceramics produced for their High-Translucency, High-Strength and High-Surface Area. *Ceramics International*, *42*(1), 1077–1085. https://doi.org/10.1016/j.ceramint.2015.09.033

Uz, M. M., Karakaş Aydınoğlu, A., & Hazar Yoruç, A. B. (2020). Effects of binder and compression strength on molding parameters of dental ceramic blocks. *Ceramics International*, *46*(8), 10186–10193. https://doi.org/10.1016/j.ceramint.2020.01.010

Xue, M., Liu, S., Wang, X., & Jiang, K. (2020). High fracture toughness of 3Y-TZP ceramic over a wide sintering range. *Materials Chemistry and Physics*, *244*(122693). https://doi.org/10.1016/j.matchemphys.2020.122693

Zhang, K., He, R., Ding, G., Feng, C., Song, W., & Fang, D. (2020). Digital light processing of 3Y-TZP strengthened ZrO2 ceramics. *Materials Science and Engineering A*, *774*(138768). https://doi.org/10.1016/j.msea.2019.138768

Zhang, Yu, & Lawn, B. R. (2019). Evaluating dental zirconia. *Dental Materials*, *35*(1), 15–23. https://doi.org/10.1016/j.dental.2018.08.291

Zhang, Y., & Lawn, B. R. (2018). Novel Zirconia Materials in Dentistry. *Journal of Dental Research*, *97*(2), 140–147. https://doi.org/10.1177/0022034517737483

Zsigmondy, R., & Scherrer, P. (1912). Bestimmung der inneren Struktur und der Größe von Kolloidteilchen mittels Röntgenstrahlen. *Kolloidchemie Ein Lehrbuch*, *277*(1916), 387–409. https://doi.org/10.1007/978-3-662-33915-2_7

Percentage of contribution of each author in the manuscript

Fabíola Stahlke Prado – 49%

Tânia Cristina Simões – 2%

Alejandra Hortencia Miranda González – 49%